**Supplemental materials**

Inventory:

3 Supplemental tables
7 Supplemental figures

**Supplemental Tables**

Supplemental Table 1. ***Prickle*** **gene expression in MTECs and mouse trachea.**

| Target | MTECs | Trachea |
|---|---|---|
| ***Prickle1*** | 1.64 | 0.96 |
| ***Prickle2*** | 23.56 | 1.85 |
| ***Prickle3*** | 0.72 | 1.00 |
| ***Prickle4*** | 7.79 | 7.58 |
| ***Centrin2*** | 8.26 | 2.21 |

Quantitative PCR for *Prickle1-4* expression in epithelial cells obtained by FACS from *Foxj1 / EGFP* MTECs (left) or trachea (right) shows that *Prickle2* and *Prickle4*, but not *Prickle1* and *Prickle3*, are enriched in EGFP+ MCCs. *Centrin2*, a ciliary gene, was used as a control for MCC-enriched expression. Gene expression was normalized to *GAPDH* control. Values represent the average of three reactions.

Supplemental Table 2. **Antibodies used**

| Protein | Catalog/clone number | Source | Dilution | Fixation* |
|---|---|---|---|---|
| **Vangl1** | HPA025235 | Sigma Aldrich | 1 to 500 | M |
| **Prickle2** | - | (1) | 1 to 200 | M |
| **ac. α-tubulin** | ab24610 | Abcam | 1 to 2,000 | M/P |
| **Foxj1** | 2A5 | eBioscience | 1 to 500 | P |
| **Muc5AC** | ab3649 | Abcam | 1 to 500 | M/P |
| **Pericentrin** | 611814 | BD Biosciences | 1 to 200 | M/P |
| **γ-tubulin** | GTU88 | Sigma Aldrich | 1 to 1,000 | M |
| **Cep83** | HPA038161 | Sigma Aldrich | 1 to 500 | M |
| **Ift88** | - | (2) | 1 to 500 | M/P |
| **Ecad** | 13-1900 | Thermo Fisher | 1 to 250 | M/P |
| **ZO1** | ZMD.437 | Thermo Fisher | 1 to 250 | M |
| **GFP** | 4745-1051 | AbD Serotech | 1 to 500 | M/P |
| **myc** | A14 | Santa Cruz Biotech | 1 to 250 | M/P |

***Fixation conditions used**

M = -20 °C methanol for 10 min at -20 °C

P = 4% paraformaldehyde for 10 min at room temperature

**References**


1. Deans MR, Antic D, Suyama K, Scott MP, Axelrod JD, and Goodrich LV. Asymmetric distribution of prickle-like 2 reveals an early underlying polarization of vestibular sensory epithelia in the inner ear. *J Neurosci.* 2007;27(12):3139-47.
2. Taulman PD, Haycraft CJ, Balkovetz DF, and Yoder BK. Polaris, a protein involved in left-right axis patterning, localizes to basal bodies and cilia. *Mol Biol Cell.* 2001;12(3):589-99.

Supplemental Table 3. **Quantitative PCR primer sequences**

| **Target** (mouse) | **Primers** | |
|---|---|---|
| ***Prickle1*** | GATGGAGAAAGCAAGCCAAG | TGTGCAGCATGGAAGAGTTC |
| ***Prickle2*** | ACATGGGCACTCTCAACTCC | TGTATCCTAGGGGGTTGCTG |
| ***Prickle3*** | TGCTGTTTCGAGTGTGAAGC | CATCACAGTATTCCGCATGG |
| ***Prickle4*** | CCACAGGACAGTGATGAACG | CCTTCAAGCTTAGGAGGCAG |
| ***Centrin2*** | ACAGGGCAGAACAAGAGCAC | CCACTGCTTATGGTGACATGG |
| ***GAPDH*** | GACTTCAACAGCAACTCCCAC | TCCACCACCCTGTTGCTGTA |

## Supplemental Figures

A

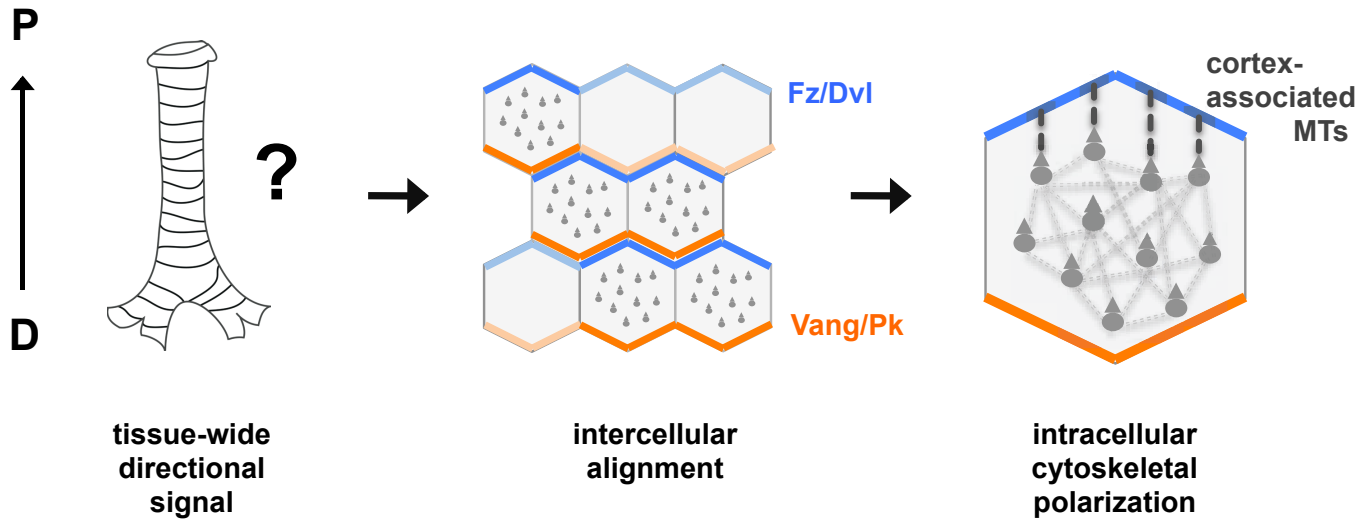
P
D
?
Fz/Dvl
Vang/Pk
cortex-associated MTs
tissue-wide directional signal
intercellular alignment
intracellular cytoskeletal polarization

B

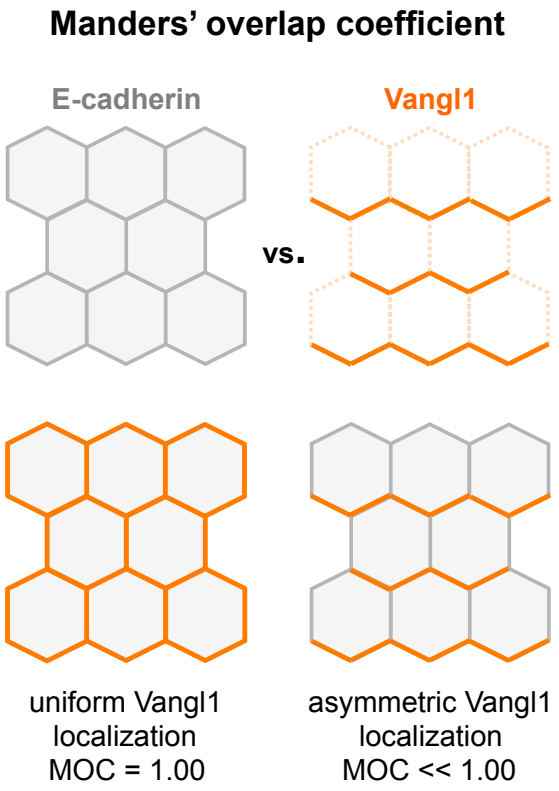
Manders' overlap coefficient
E-cadherin
Vangl1
vs.
uniform Vangl1 localization
MOC = 1.00
asymmetric Vangl1 localization
MOC << 1.00

C

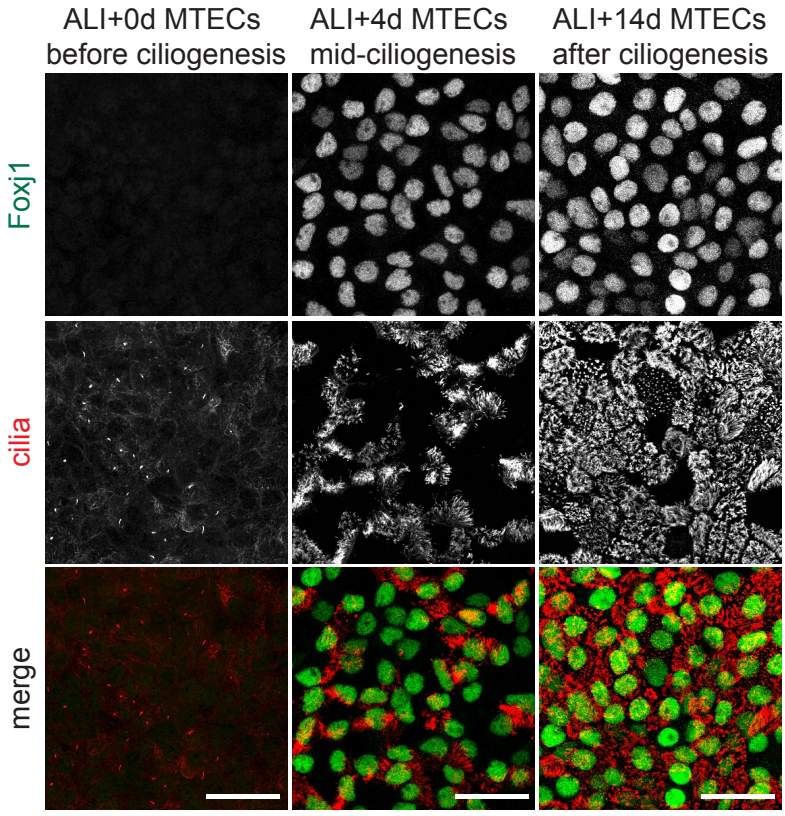
ALI+0d MTECs before ciliogenesis
ALI+4d MTECs mid-ciliogenesis
ALI+14d MTECs after ciliogenesis
Foxj1
cilia
merge

**D**

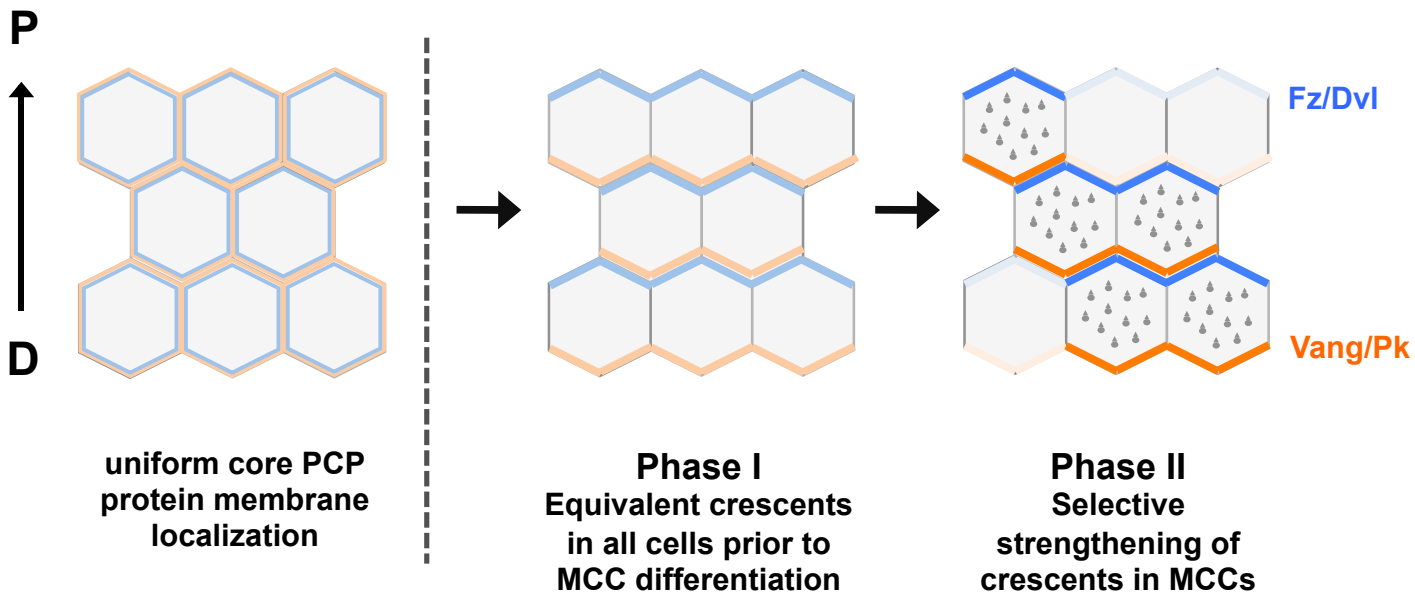


Supplemental Figure 1. **Planar cell polarity (PCP) signaling and motile ciliogenesis in airway epithelial cells. (A)** Schematic of the PCP signaling mechanism in the airways. As yet unknown global directional cues specify the proximal-distal (P-D) polarity axis. The core PCP signaling cassette is responsible for the local coordination and propagation of cell polarities. Intercellular communication across adjacent cell boundaries occurs by mutual recruitment between the Fz/Dvl (proximal) and Vangl/Prickle (Pk) (distal) complexes. Within multiciliated cells (MCCs), cytoskeletal elements (light grey dotted lines) link individual cilia to each other and cortex-associated microtubules (MTs, dark grey dotted lines) tether the cilia to the proximal side Fz/Dvl crescent for directional motility. (**B)** Schematic of the Manders' overlap coefficient (MOC) metric for Vangl1 crescent asymmetric localization. The MOC indicates the extent of overlap between Vangl1 and E-cadherin (Ecad), which marks the entire adherens junctional domain. A MOC of 1.00 indicates completely uniform Vangl1 localization, whereas values less than 1.00 point to asymmetric Vangl1 localization. (**C)** Mouse tracheal epithelial cells (MTECs) undergoing differentiation labeled with Foxj1 (green) and ac. α-tubulin (cilia, red) antibodies show that ciliogenesis has not yet occurred at air-liquid interface (ALI) +0 days (left). There is active ciliogenesis at ALI+4 days (middle) and ciliogenesis is complete by ALI+14 days (right). Nuclear Foxj1 is an earlier marker of motile ciliogenesis than the appearance of ac. α-tubulin labeling of motile cilia. Images representative of $n$ > 10 MTEC timecourses. Scale bar, 25 μm. (**D)** Schematic of the 2 phases of core PCP protein crescent acquisition in multiciliated airway epithelial cells. Upon epithelialization, core PCP proteins are targeted to the apical junctional membrane and are briefly uniformly localized. Prior to MCC differentiation, core PCP proteins engage in intercellular communication to assemble into P-D oriented crescents of equivalent intensity in all cells. After MCC differentiation, PCP crescents are consolidated in MCCs and motile cilia align with the P-D axis.

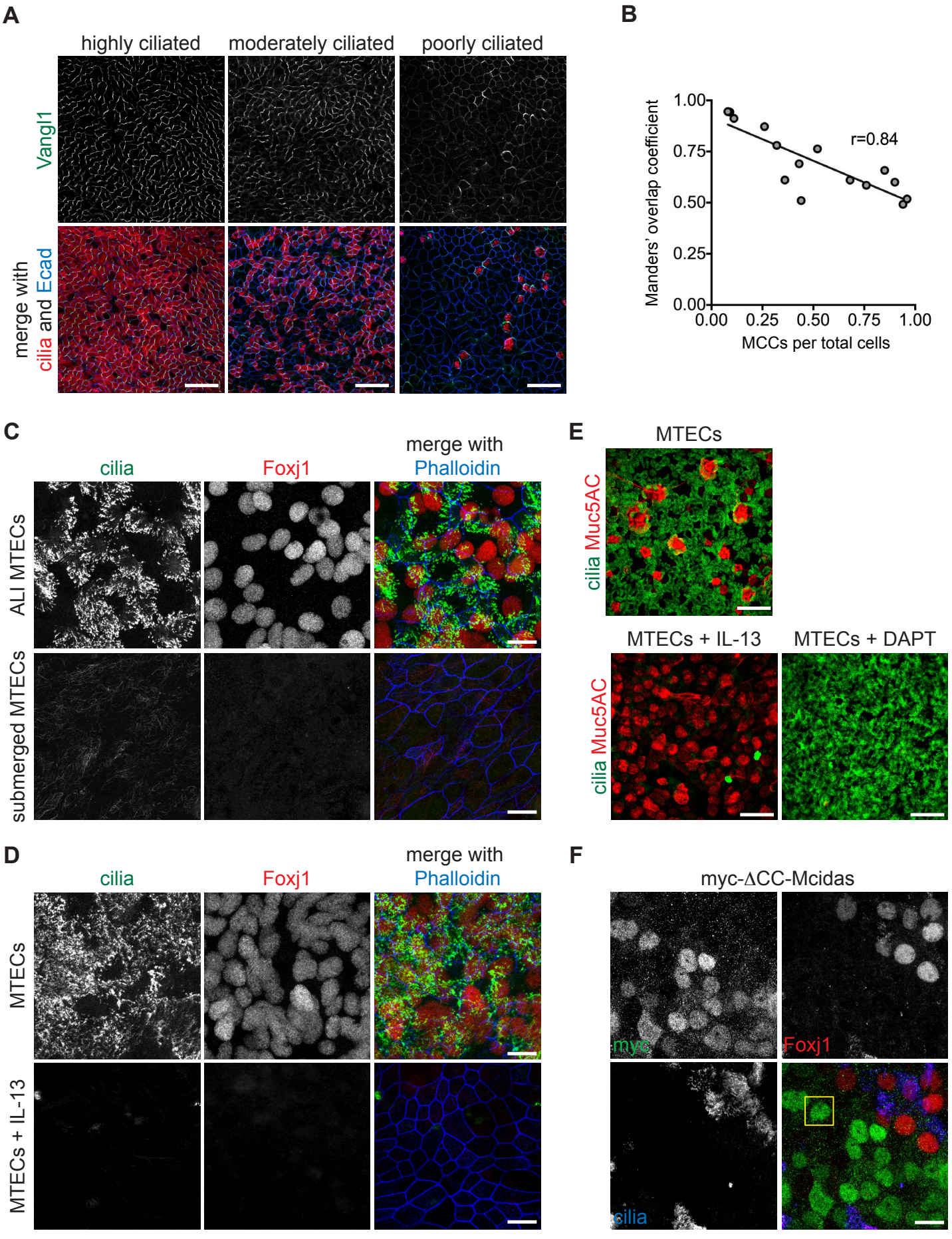
A
highly ciliated
moderately ciliated
poorly ciliated
Vangl1
merge with
cilia and Ecad
B
Manders' overlap coefficient
1.00
0.75
0.50
0.25
0.00
r=0.84
0.00 0.25 0.50 0.75 1.00
MCCs per total cells
C
cilia
Foxj1
merge with
Phalloidin
ALI MTECs
submerged MTECs
E
MTECs
cilia Muc5AC
MTECs + IL-13
MTECs + DAPT
cilia Muc5AC
D
cilia
Foxj1
merge with
Phalloidin
MTECs
MTECs + IL-13
F
myc-ΔCC-Mcidas
myc
Foxj1
cilia

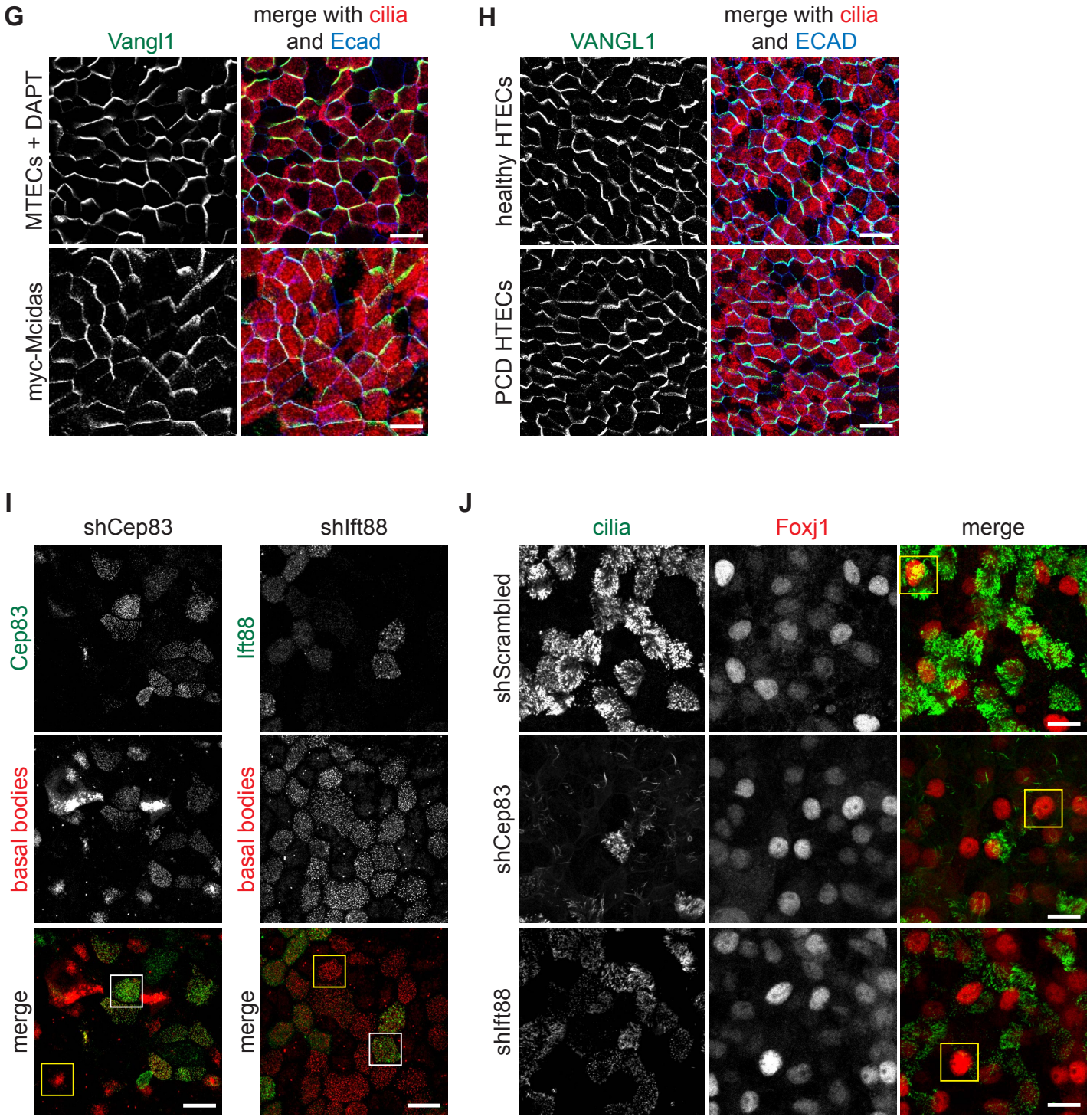


Supplemental Figure 2. **Interfering with MCC differentiation blocks Vangl1 asymmetric localization. (A)** ALI+14 days MTECs labeled with Vangl1 (green), ac. α-tubulin (cilia, red) and Ecad (blue) antibodies show that only well-ciliated MTECs have robust Vangl1 crescents. **(B)** Fraction of MCCs per total cells and Vangl1 MOC were calculated for *n* = 15 images of ALI+14 days MTECs labeled with Vangl1, ac. α-Tubulin and Ecad. Paired values were plotted, and a trendline was generated using linear regression to show that Vangl1 MOC increases as MCC fraction increases (Pearson correlation, r = 0.84, *P* < 0.001). **(C)** MTECs cultured submerged for 5+14 days (control MTECs were cultured submerged for 5, then at ALI for 14 days), and then labeled with ac. α-tubulin (cilia, green) and Foxj1 (red) antibodies and stained with Phalloidin to mark cell boundaries (blue) show that MCC fate acquisition is blocked by submerged culture. **(D)** MTECs treated with IL-13 from ALI+0 to +14 days and labeled with ac. α-tubulin (cilia, green) and Foxj1 (red) antibodies and stained with Phalloidin to mark cell boundaries (blue) show that MCC fate acquisition is blocked by IL13 treatment. **(E)**

MTECs treated with IL-13 or DAPT from ALI+0 to +14 days and labeled with ac. α-tubulin (cilia, green) and Muc5AC (red) antibodies to mark cilia and mucins, show that untreated cultures (top) contain mainly MCCs, while IL-13 treatment (bottom left) promotes the differentiation of mucus secreting cells and DAPT treatment (bottom right) promotes the differentiation of MCCs. **(F)** MTECs infected with lentivirus containing myc-tagged ΔCC-Mcidas at day 4 of culture were labeled at ALI+14 days with anti-myc (green), Foxj1 (red) and ac. α-tubulin (cilia, blue) antibodies. Myc+ cells always lack Foxj1 signal, indicating that MCC fate acquisition is blocked by myc-ΔCC-Mcidas expression. **(G)** MTECs treated with DAPT (top) from ALI+0 to 14 days and labeled with Vangl1 (green), ac. α-tubulin (cilia, red) and Ecad (blue) antibodies show that Vangl1 is robustly asymmetric when MCC differentiation is promoted by Notch inhibition. Compare to Fig. 2B for untreated MTECs. MTECs infected with lentivirus containing full length Mcidas (bottom) at day 4 of culture and labeled at ALI+14 days with Vangl1 (green), ac. α-tubulin (cilia, red) and Ecad (blue) antibodies show that Vangl1 is robustly asymmetric when MCC differentiation is promoted by Mcidas expression. Compare to Fig. 2C for GFP alone infected MTECs. **(H)** Human tracheal epithelial cells (HTECs) generated from healthy (top) and primary ciliary dyskinesia (PCD, bottom) donor tissue and labeled at ALI+30 days with VANGL1 (green), ac. α-tubulin (cilia, red) and ECAD (blue) antibodies show that PCD cultures have robust VANGL1 crescents. Image representative of phenotype observed in *n* = 3 distinct donors. **(I)** MTECs infected with lentivirus containing Cep83 (left) or Ift88 (right) shRNA at day 4 of culture were labeled at ALI+14 days with anti-Cep83 (green, left) or Ift88 (green, right) and Pericentrin (basal bodies, red, left) or γ-tubulin (basal bodies, red, right) antibodies. Cep83-depleted cells (yellow box) show undocked, clustered Cep83-negative basal bodies, while uninfected cells (white box) show fully docked and dispersed, Cep83-positive basal bodies. Ift88-depleted cells (yellow box) show fully docked and dispersed basal bodies and no Ift88 signal from cilia, while uninfected cells (white box) show fully docked and dispersed basal bodies and Ift88 signal from cilia. **(J)** MTECs infected with lentivirus containing scrambled sequence (top), Cep83 (middle) or Ift88 (bottom) shRNA at day 4 of culture were labeled at ALI+14 days with ac. α-tubulin (cilia, green) and Foxj1 (red) antibodies to show that MCC fate acquisition is not affected by the lentiviral RNAi. Scale bars, 75 μm (A,C),10 μm (D-J). Images in C-G and I,J are representative *n* = 3 lentiviral infection or drug treatment of MTECs.

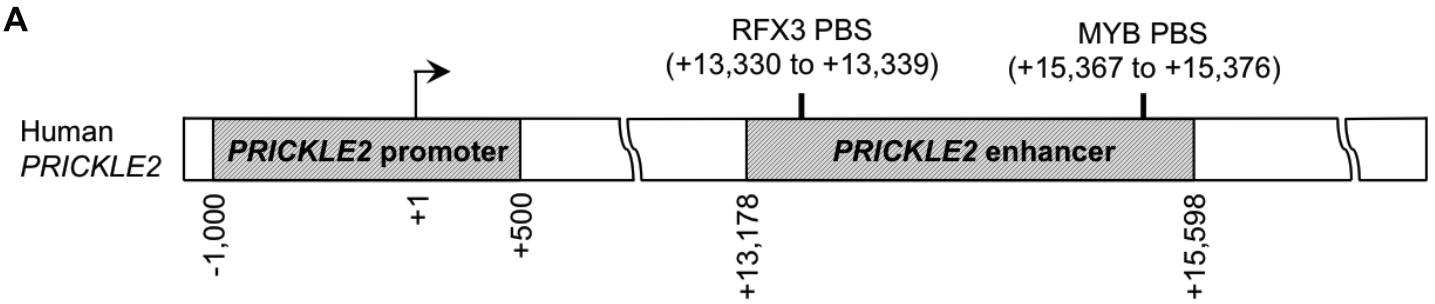
A
RFX3 PBS
(+13,330 to +13,339)
MYB PBS
(+15,367 to +15,376)
Human
PRICKLE2
PRICKLE2 promoter
PRICKLE2 enhancer
-1,000
+1
+500
+13,178
+15,598

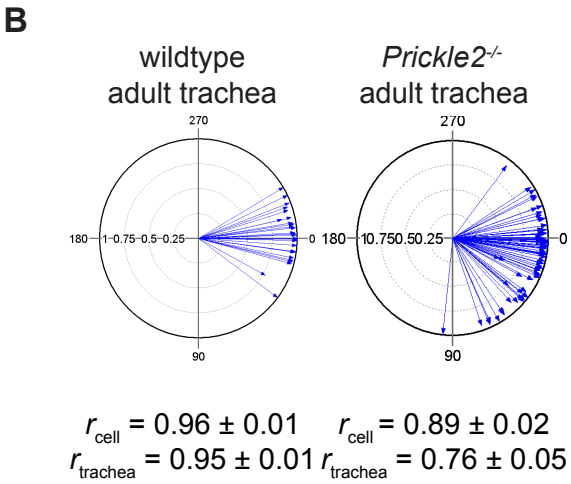
B
wildtype
adult trachea
Prickle2-/-
adult trachea
270
180
0
90
$r_{cell}$ = 0.96 ± 0.01
$r_{trachea}$ = 0.95 ± 0.01
$r_{cell}$ = 0.89 ± 0.02
$r_{trachea}$ = 0.76 ± 0.05

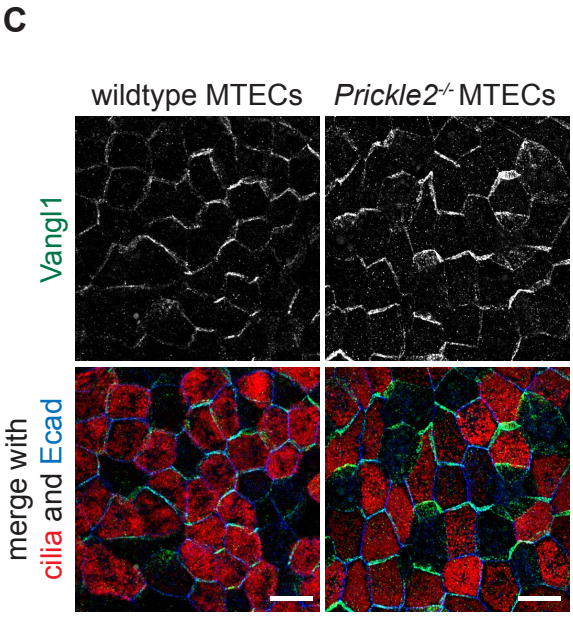
C
wildtype MTECs
Prickle2-/- MTECs
Vangl1
merge with
cilia and Ecad

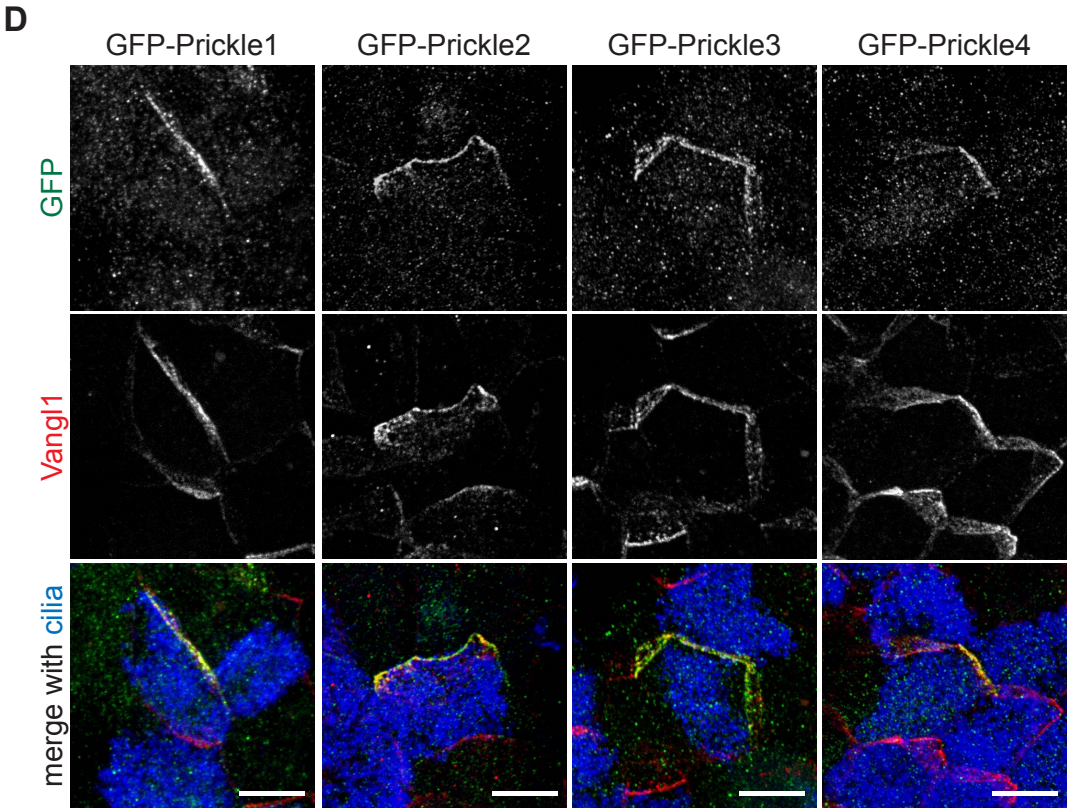
D
GFP-Prickle1
GFP-Prickle2
GFP-Prickle3
GFP-Prickle4
GFP
Vangl1
merge with cilia

Supplemental Figure 3. **Prickle expression in airway epithelial cells. (A)** Schematic showing the human *PRICKLE2* promoter and enhancer genomic fragments tested in the luciferase assay. The *PRICKLE2* enhancer region contains a MYB and an RFX3 predicted binding site (PBS). **(B)** Circular plots showing basal body orientation in adult wildtype and *Prickle2*$^{-/-}$ mice demonstrate that intracellular basal body alignment ($r_{cell}$) is not significantly different (two-tailed Student's *t* test), but global basal body alignment ($r_{trachea}$) is reduced (two-tailed Student's *t* test, $P < 0.05$) in the mutants compared to wildtype. Circular plots show data from a representative individual, circular statistics calculated from $n = 3$ mice. **(C)** ALI+14 days wildtype and *Prickle2*$^{-/-}$ MTECs were labeled with Vangl1 (green), ac. α-tubulin (cilia, red) and Ecad (blue) antibodies both show robust Vangl1 crescents. Images are representative of cultures from $n = 3$ *Prickle2*$^{-/-}$ mice and littermate controls. **(D)** MTECs infected with *GFP-Prickle1-4* containing lentivirus labeled with GFP (green), Vangl1 (red) and ac. α-tubulin (cilia, blue) antibodies show that all four GFP-tagged Prickles localize asymmetrically in MCCs. Images are representative of $n = 3$ lentiviral infections of MTECs. Scale bars, 10 μm (C), 5 μm (D).

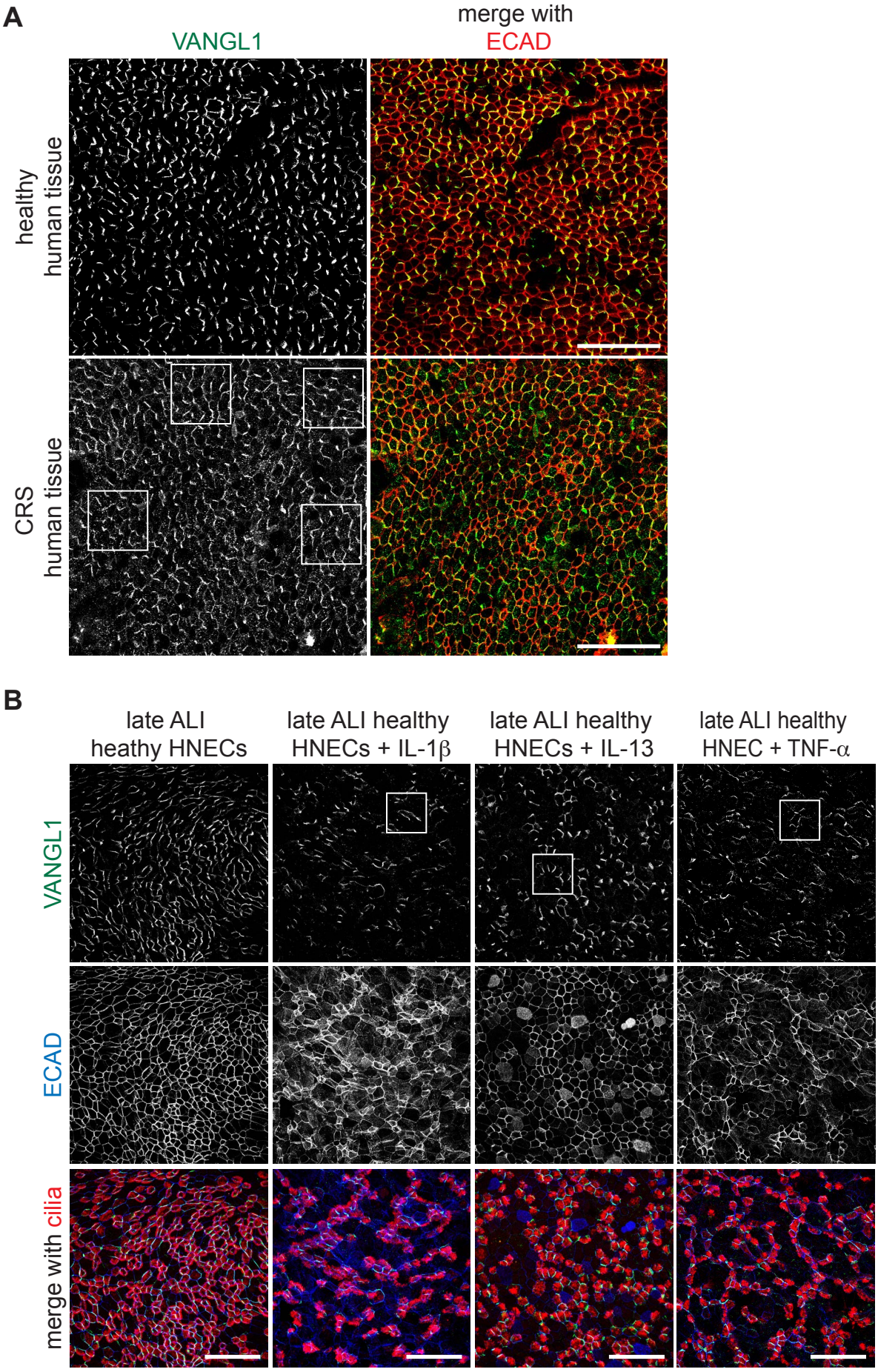
A
VANGL1
merge with
ECAD
healthy
human tissue
CRS
human tissue
B
late ALI
heathy HNECs
late ALI healthy
HNECs + IL-1β
late ALI healthy
HNECs + IL-13
late ALI healthy
HNEC + TNF-α
VANGL1
ECAD
merge with cilia

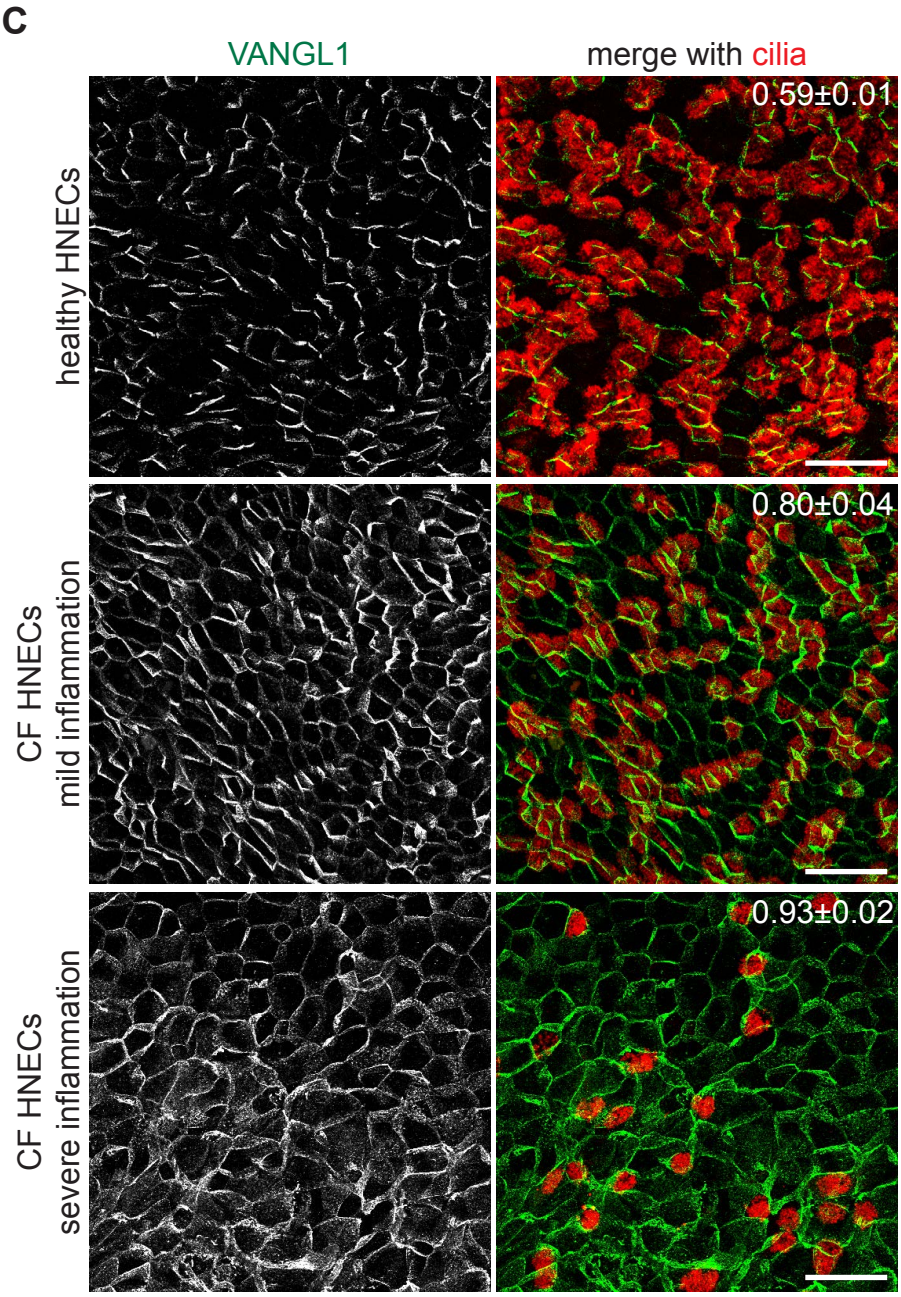


Supplemental Figure 4. **VANGL1 localization is abnormal in diseased human airway epithelia. (A)** Healthy (top) and chronic rhinosinusitis (CRS, bottom) human sinonasal tissue labeled with VANGL1 (green) and ECAD (red) antibodies shows that every VANGL1 crescent is located on the same side of each cell along the tissue axis in the healthy tissue, but VANGL1 crescents do not all show long range polarity coordination in CRS (boxed areas). Images are representative of samples from *n* = 3 CRS donors. **(B)** Fully differentiated healthy human nasal epithelial cells (HNECs) treated with IL-1β, IL-13 and TNF-α from ALI+30 to +40 days and labeled with VANGL1 (green), ac. α-tubulin (cilia, red) and ECAD (blue) antibodies show that VANGL1 is still fully asymmetrically localized in MCCs (boxed areas). Images are representative of *n* = 3 drug treatments of HNECs from *n* = 3 donors. **(C)** Healthy HNECs (top) and CF HNECs generated from donor tissue showing mild (middle) or severe (bottom) inflammation and labeled with VANGL1 (green) and ac. α-tubulin (cilia, red) antibodies show that overt inflammation correlates with degree of MCC loss and disruption of VANGL1 asymmetric localization. Images are representative of samples from *n* = 3 CF donors. Manders' overlap coefficient ± standard error indicated on merged images. Scale bars, 50 μm (A-B), 25 μm (C).

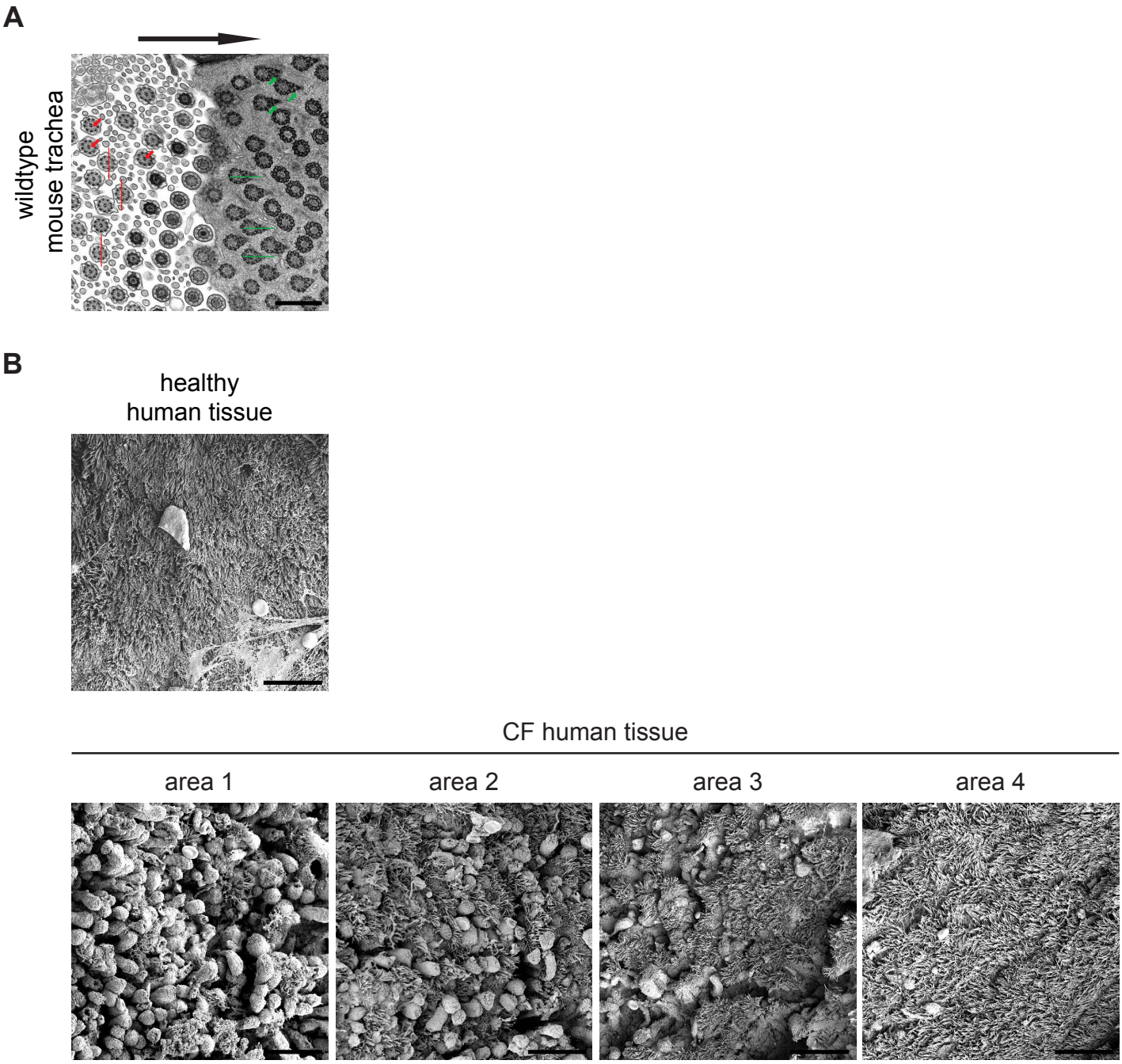


Supplemental Figure 5. **Human CF sinonasal epithelium has abnormal MCCs. (A)** Transmission electron microscopy of mouse tracheal epithelium (arrow shows proximal or oral direction); motile cilium beat direction is indicated by the direction in which basal feet point (green arrows point to some basal feet; green lines drawn through others) or by the direction perpendicular to a line drawn through the central axonemal microtubule doublet (red arrows point to some central doublets; red lines pass through some others). **(B)** Scanning electron microscopy shows robustly ciliated healthy human sinonasal epithelium (top) and nearly normal to absent MCCs in different regions of a CF tissue (bottom, area 1-4). Cilia appear less well-organized even in robustly ciliated areas. Hyperplasia of mucus secreting cells (recognized by domed apical surface) at the expense of MCCs is evident in areas 1 and 2. Images are representative of samples from *n* = 3 donors. Scale bar, 1 μm (A), 20 μm (bottom).

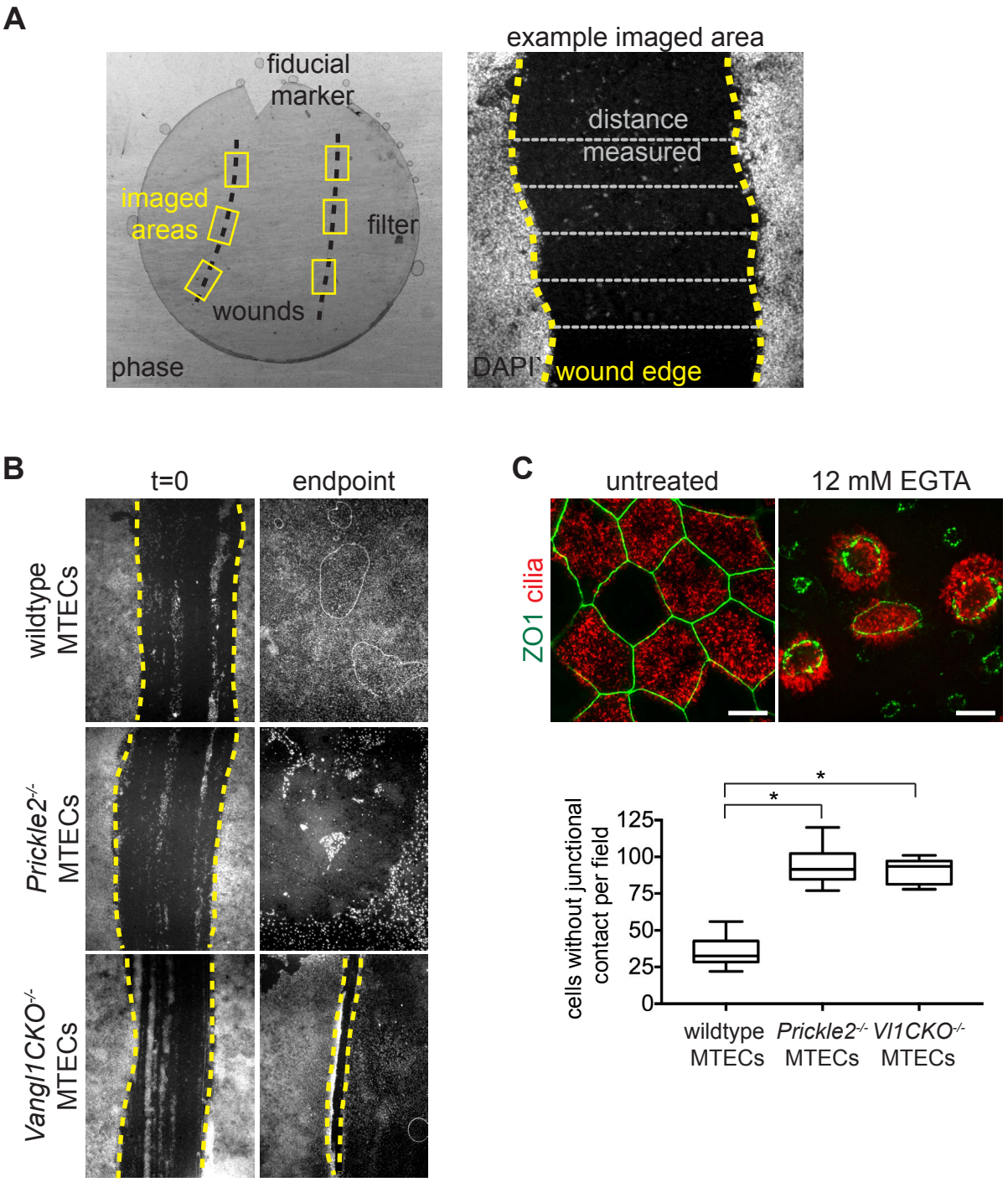


Supplemental Figure 6. **PCP mutant MTECs have impaired barrier function and wound healing. (A)** Low magnification image of a Transwell filter (left) and higher magnification image of a freshly created wound (t=0, right) indicate wound and measurement areas for the MTEC/HNEC scratch wound assay. Wound edges are identified based on DAPI staining. **(B)** Wildtype, *Prickle2*$^{-/-}$ and *Vangl1CKO*$^{-/-}$ MTECs scratch wounded in triplicate at ALI+14 days of culture (t=0) and allowed to regenerate for 48h (end point). **(C)** ALI+14 day wildtype MTECs were treated with 12 mM EGTA for 30 mins and labeled with anti-ZO1 (tight junctions, green) and ac. α-tubulin (cilia, red) antibodies to mark apical junctions and cilia. ZO1 labeling shows intact (left) and dissociated (right) junctions. For junctional integrity assay, wildtype, *Prickle2*$^{-/-}$ and *Vangl1CKO*$^{-/-}$ MTECs were treated with 12 mM EGTA for 10 mins and in triplicate experiments cells without junctional contact per frame were counted based on ZO1 labeling in $n$ = 10 frames. Box and whisker plot shows the minimum, lower quartile, median, upper quartile and maximum values. One-way ANOVA with post hoc Dunnett's multiple comparison test; *$P$ < 0.0001. Scale bars, 5 μm (C).

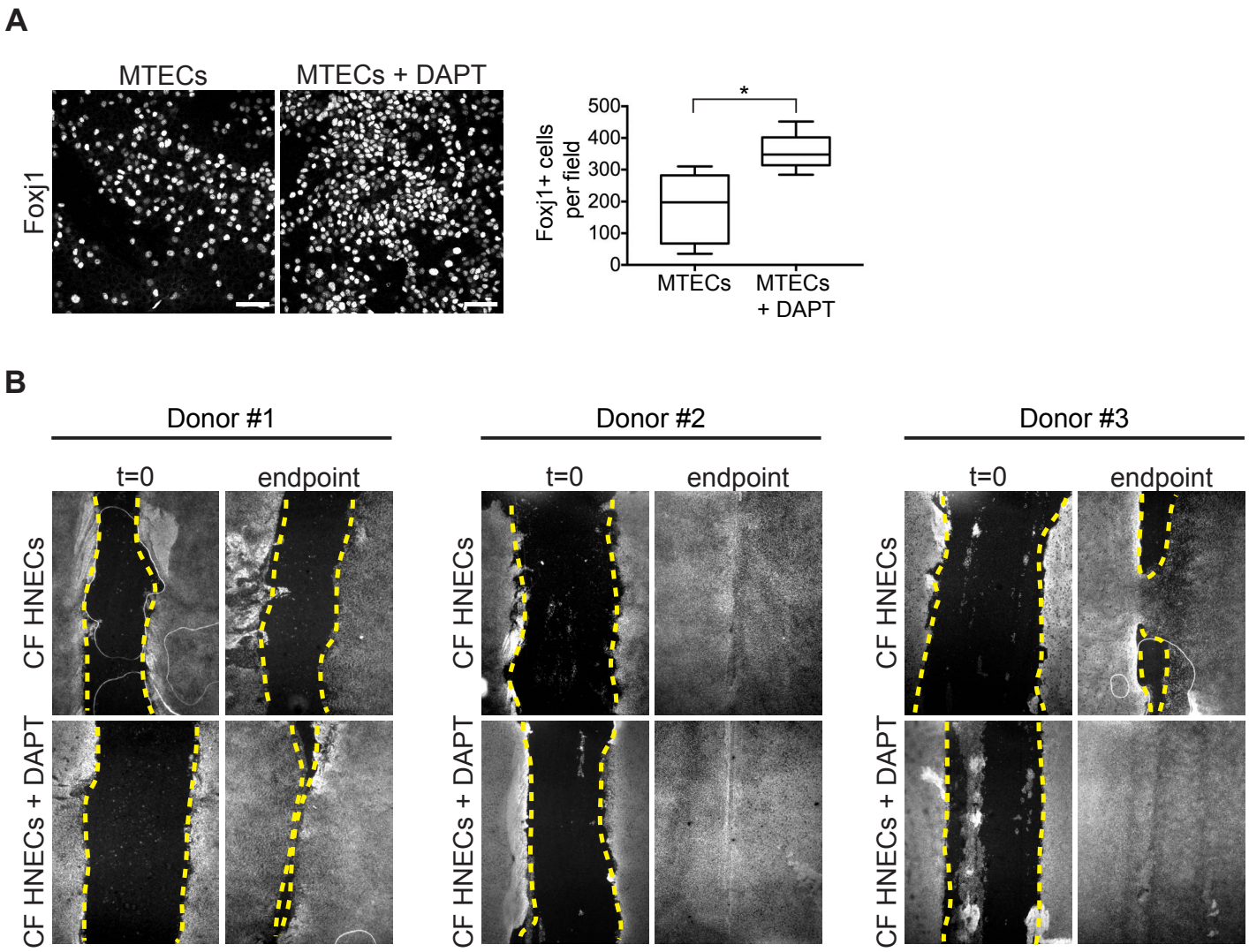


Supplemental Figure 7. **Notch inhibition improves epithelial function in CF HNECs. (A)** MTECs were treated with DAPT from ALI+0 to 4 days, then labeled with Foxj1 antibody to mark MCCs. Foxj1+ cells were counted in *n* = 10 fields in triplicate. Box and whisker plot shows the minimum, lower quartile, median, upper quartile and maximum values. Two-tailed Student's *t* test; **P* < 0.001. **(B)** Untreated and DAPT-treated CF HNECs from *n* = 3 donors were scratch wounded at ALI+30 days of culture (t=0) and allowed to regenerate for 48h (end point). Scale bar, 25 μm.